Modeling phototrophic biofilms in a plug-flow reactor

J. D. Muñoz Sierra, C. Picioreanu and M. C. M. van Loosdrecht

ABSTRACT

The use of phototrophic biofilms in wastewater treatment has been recognized as a potential option for development of new reactor configurations. For better understanding of these systems, a numerical model was developed including relevant microbial processes. As a novelty, this model was implemented in COMSOL Multiphysics, a modern computational environment for complex dynamic models. A two-dimensional biofilm model was used to study the spatial distribution of microbial species within the biofilm and along the length of the reactor. The biofilm model was coupled with a one-dimensional plug-flow bulk liquid model. The impact of different operational conditions on the chemical oxygen demand (COD) and ammonia conversions was assessed. The model was tuned by varying two parameters: the half-saturation coefficient for light use by phototrophs and the oxygen mass transfer coefficient. The mass transfer coefficient was found to be determining for the substrate conversion rate. Simulations indicate that heterotrophs would overgrow nitrifiers and phototrophs within the biofilm until a low biodegradable COD value in the wastewater is reached (organic loading rate <2.32 gCOD/(m^2 d)). This limits the proposed positive effect of treating wastewater with a combination of algae and heterotrophs/autotrophs. Mechanistic models like this one are made for understanding the microbial interactions and their influence on the reactor performance.

Key words | algae–bacteria, bioreactor, COMSOL, modeling, phototrophic biofilms

J. D. Muñoz Sierra (corresponding author)
C. Picioreanu
M. C. M. van Loosdrecht
Department of Biotechnology,
Delft University of Technology,
Julianalaan 67, 2628 BC,
Delft,
The Netherlands
E-mail: *J.D.MunozSierra@tudelft.nl*

J. D. Muñoz Sierra
Department of Water Management,
Delft University of Technology,
Stevinweg 1, 2628 CN,
Delft,
The Netherlands

M. C. M. van Loosdrecht
KWR Watercycle Research Institute,
P.O. Box 1072,
3430 BB,
Nieuwegein,
The Netherlands

INTRODUCTION

In general, regulations for wastewater treatment are becoming stricter over the world, especially for compounds such as nitrogen and phosphorus (Boelee *et al.* 2011). For this purpose reactors utilizing phototrophic biofilms have been recognized as a promising wastewater treatment option (Safonova *et al.* 2004; Muñoz & Guieysse 2006; Roeselers *et al.* 2008). Microalgae can take up nitrogen and phosphorus using inorganic carbon as carbon source, and natural or artificial light as energy source. Also, algae and bacteria provide each other with oxygen and carbon dioxide in a symbiotic relationship. For these reasons, algae–bacteria-based processes can be to a certain extent a more environmentally friendly and less energy-demanding option when compared to conventional treatment technologies. The photosynthetic activity in the biofilm community leads to oxygen production and nutrient uptake for biomass formation (Wilkie & Mulbry 2002; González *et al.* 2008). There is an increased interest in the use of attached phototrophic communities growing on different surfaces and using different reactor configurations (Schumacher & Sekoulov 2002; Shi *et al.* 2007), either as a polishing system for the wastewater or as a cradle for biofuels and bioproducts production (Christenson & Sims 2011). Bioreactors based on algae–bacteria growth in biofilms have been reported to exhibit high treatment efficiencies (Borde *et al.* 2003; Chavan & Mukherji 2008, 2010; De Godos *et al.* 2009).

Up to now, minor attention has been given to the possibility of using algae–bacteria biofilms for a complete sewage treatment. The challenge is to accomplish high organic matter and nutrient removals using the minimum land and energy resources. The algae–bacteria-based system uses a low light intensity to be less energy-demanding than other treatment methods (e.g. aeration). Therefore, a better understanding of the dynamics of phototropic

doi: 10.2166/wst.2014.368

biofilm communities is essential in order to optimize the performance of the application and technology development. The efficiency and reliability of phototrophic biofilm reactors depend to a certain extent on the possibility to select and keep desired community compositions (Roeselers *et al.* 2008).

This study aims at creating a mechanistic numerical model to describe the dynamics of microbial populations in a mixed biofilm community with heterotrophic, nitrifying and phototrophic activity. The biofilm model is integrated in a bioreactor model with plug-flow wastewater.

MATERIALS AND METHODS

Model description

The goal of the model is to describe the dynamics of overall chemical oxygen demand (COD) and ammonium removal rates in a phototrophic biofilm reactor operated in plug-flow configuration. This biofilm model provides information at both macro- and micro-scale. Important macro-scale outputs are the substrate (COD and NH_4) removal rates and biomass loss from the system. Micro-scale model outputs include the spatial distribution of substrates and microbial communities both within the biofilm and along the reactor flow path.

Model geometry, dimensions and compartments

The model assumes a two-dimensional (2D) biofilm, with properties varying in the biofilm depth (z direction) and along the bioreactor (x direction). The biofilm has a fixed thickness L_B (500 μm), and it is attached to an impermeable flat surface. The biofilm develops on trays along a plug-flow of water measuring $L_R = 9$ m. The 2D biofilm compartment is coupled to a one-dimensional (1D) bulk liquid model (Figure 1) so that chemical species can be exchanged between these two domains.

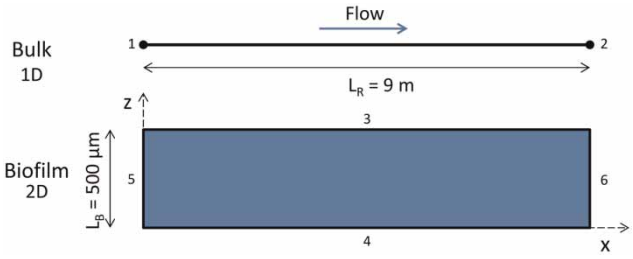

Figure 1 | Model geometry and coupling between the 2D biofilm and 1D bulk liquid compartments. 1: liquid inlet, 2: liquid outlet, 3: biofilm surface coupled with the bulk liquid model, 4, 5, and 6: insulation boundaries (no-flux).

Components and state variables

Multispecies biofilm models for phototrophic systems should include algae–bacteria consortia. Several metabolisms (i.e., aerobic, anoxic, or anaerobic) play a role according to the redox potential and interactions within communities. Therefore, three kinds of essential functional groups of microorganisms are considered: phototrophic (Ph), heterotrophic (Het) and autotrophic (nitrifying, Aut). In addition, inert particulate compounds (I), which result from decay processes, are also included. The solutes considered are organic matter (S, COD), ammonium ($N\text{-}NH_4$), oxygen (O_2), and inorganic carbon (CO_2). Consequently, the model state variables are divided into soluble (S_i) and particulate (X_i) matter, following the approach used in Activated Sludge Models (ASM) (Henze *et al.* 2000) and the PHOBIA Model (Wolf *et al.* 2007).

Processes

Inside the phototrophic system the solutes are transported and react, leading to biofilm growth. The microbial processes considered in this model are growth, respiration and inactivation of phototrophic, heterotrophic and nitrifying microorganisms. To maintain this initial model within reasonable limits of complexity, other potential processes (such as production of internal or external storage compounds by algae) have been neglected. The stoichiometry of microbial processes is presented in Table 1 and reaction rates in Table 2. All model parameters are listed in the supplementary material, Table S1 (available online at http://www.iwaponline.com/wst/070/368.pdf).

The nitrogen source is ammonia, and CO_2 is the only carbon source for phototrophic growth. Acid–base equilibria have been neglected and sufficient buffer (keeping a constant pH) has been assumed in the wastewater. The biomass inactivation leads to inert X_I, similar to ASM1 (Henze *et al.* 2000). The rate of photosynthetic growth in this model does not include inhibition because of the relatively low light intensity assumed. The light attenuation

Table 1 | Stoichiometry matrix of the microbial processes in the model

	Particulate components				Soluble components				
Processes	X_{Het} gCOD/m³	X_{Aut} gCOD/m³	X_{Ph} gCOD/m³	X_I gCOD/m³	S_S gCOD/m³	S_{NH4} gN/m³	S_{O2} gO_2/m^3	S_{CO2} gCO_2/m^3	Rates
Heterotrophs growth	1				$\frac{-1}{Y_H}$	0.083	$1-\frac{\alpha_H}{Y_H}$	$\frac{1}{Y_H}-0.952$	r1
Heterotrophs inactivation	−1			1					r2
Heterotrophs respiration	−1						−1		r3
Autotrophs (nitrifiers) growth		1				$\frac{-1}{Y_N}$	$1-\frac{\alpha_N}{Y_N}$	−1.309	r4
Autotrophs inactivation		−1		1					r5
Autotrophs respiration		−1					−1		r6
Phototrophs growth on ammonium and CO_2			1			0.074	0.094	−1.378	r7
Phototrophs inactivation			−1	1					r8
Phototrophs respiration			−1				−1		r9

Table 2 | Rate expressions of the microbial processes

	Rates
r1	$\mu_{\max,\mathrm{Het}}\cdot\left(\frac{S_S}{K_{s,S,\mathrm{Het}}+S_S}\cdot\frac{S_{O_2}}{K_{s,O_2,\mathrm{Het}}+S_{O_2}}\right).X_{\mathrm{Het}}$
r2	$b_{ina,\mathrm{Het}}.X_{\mathrm{Het}}$
r3	$b_{res,\mathrm{Het}}\cdot\left(\frac{S_{O_2}}{K_{s,O_2,\mathrm{Het}}+S_{O_2}}\right).X_{\mathrm{Het}}$
r4	$\mu_{\max,\mathrm{Aut}}\cdot\left(\frac{S_{CO_2}}{K_{s,CO_2,\mathrm{Aut}}+S_{CO_2}}\cdot\frac{S_{O_2}}{K_{s,O_2,\mathrm{Aut}}+S_{O_2}}\cdot\frac{S_{NH_4}}{K_{s,NH_4,\mathrm{Aut}}+S_{NH_4}}\right).X_{\mathrm{Aut}}$
r5	$b_{ina,\mathrm{Aut}}.X_{\mathrm{Aut}}$
r6	$b_{res,\mathrm{Aut}}\cdot\left(\frac{S_{O_2}}{K_{s,O_2,\mathrm{Aut}}+S_{O_2}}\right).X_{\mathrm{Aut}}$
r7	$\mu_{\max,Ph}\cdot\left(\frac{S_{CO_2}}{K_{s,CO_2,Ph}+S_{CO_2}}\cdot\frac{I}{K_{s,I,Ph}+I}\cdot\frac{S_{NH_4}}{K_{s,NH_4,Ph}+S_{NH_4}}\right).X_{Ph}$
r8	$b_{ina,Ph}.X_{Ph}$
r9	$b_{res,Ph}\cdot\left(\frac{S_{O_2}}{K_{s,O_2,Ph}+S_{O_2}}\right).X_{Ph}$

across the biofilm follows the Lambert–Beer equation function of total biomass density in the biofilm

$$I(z) = I_{\mathrm{in}}.\, e^{-k_{\mathrm{tot}}(L_B-z)\sum_i X_i}$$

Bulk liquid

The 1D mass balance equation for each solute i in the bulk liquid allows calculation of $S_{i,L}(t,x)$ and includes convective transport due to water flow along the reactor (constant

velocity u_L), the flux exchanged with the biofilm $R_{i,LB}$, and, only for oxygen, a gas–liquid transfer rate $R_{i,GL}$. Biological and chemical conversion processes in the bulk liquid $R_{i,L}$ have been neglected.

$$\frac{\partial S_{i,L}}{\partial t} + u_L \frac{\partial S_{i,L}}{\partial x} = R_{i,LB} + R_{i,GL}$$

The bulk–biofilm exchange rate is based on the diffusive flux to/from the biofilm (Fick's first law)

$$R_{i,LB} = J_i A_B = -A_B D_{i,B} \frac{\partial S_{i,B}}{\partial z},$$

where $D_{i,B}$ is the diffusion coefficient of the solute in the biofilm, and A_B is the biofilm specific surface area. In this mass balance, the gas–liquid oxygen transfer is $R_{O_2,GL} = k_{La}\left(S^*_{O_2} - S_{O_2,L}\right)$, with k_{La} the mass transfer coefficient.

In accordance with Pasztor *et al.* (2009), an inert COD fraction of 25% in the wastewater was assumed.

Biofilm

Each solute i diffuses (diffusion coefficient $D_{i,B}$) and reacts (net rate $R_{i,B}$) in the 2D biofilm, and concentrations $S_{i,B}(t, x,z)$ are calculated from the following equation:

$$\frac{\partial S_{i,B}}{\partial t} = D_{i,B}\left(\frac{\partial^2 S_{i,B}}{\partial x^2} + \frac{\partial^2 S_{i,B}}{\partial z^2}\right) + R_{i,B}$$

The net rate $R_{i,B}$ is calculated by the sum of all microbial process rates (Table 2) multiplied by the respective stoichiometry coefficient (Table 1). Initial concentrations ($t = 0$) of all species were assumed the same in biofilm and bulk liquid, and equal to inlet ($x = 0$) concentrations $S_{i,L} = S_{i,L,in}$. The concentrations in the bulk liquid compartment constitute the boundary condition at the biofilm surface ($z = L_B$) for the biofilm compartment, with values changing over time. The other three biofilm boundaries (Figure 1) are zero flux (insulation) for all solutes.

The transport by advection and formation of each biomass component j in the biofilm is described by another mass balance, from which $X_{j,B}(t,x,z)$ is calculated

$$\frac{\partial X_{j,B}}{\partial t} + u_B \frac{\partial X_{j,B}}{\partial z} = R_{j,B}.$$

In this case, the advective velocity (u_B) of the particulate component is expressed in the direction z (i.e., perpendicular to the substratum) and no biomass transport is considered over the x direction. Similar to Wanner & Reichert (1996), the advective velocity of biomass, $u_B(z)$, is computed from

$$\frac{du_B}{dz} = \frac{\sum_j R_{j,B}}{X_{\text{Total}}}.$$

At the biofilm base $z = 0$, the advective velocity is zero, $u_B(z) = 0$. All the solute rates ($R_{i,B}$) depend on the local microbial rates $R_{j,B}(t,x,z)$ for the different microorganisms.

For simulations describing competition between microbial species, the type of biomass detachment chosen has an important influence on model predictions (Morgenroth & Wilderer 2000). In the current model, we adopted the simplifying assumption of a continuous biomass detachment that leads to constant biofilm thickness. This is acceptable for the present model purposes, as shown in previous studies (Wanner & Gujer 1985; Ohashi *et al.* 1995; Wanner & Reichert 1996).

Model solution

Models were implemented in COMSOL Multiphysics 4.2a (Comsol Inc., Burlington, MA, www.comsol.com). Other computational tools (such as AQUASIM software, Wanner & Reichert (1996)) could also be used for this purpose, with more or less adaptations needed. In AQUASIM the system would be represented as a series of continuos stirred tank reactor compartments with biofilm. However, due to the plug-flow (i.e., the channel of 9 m is much longer than the liquid height above the biofilm of 1 cm), many of such compartments would have to be used, which complicates the model construction and results representation. COMSOL on the other hand presents the advantage of a total flexibility in choosing model structure, model equations and domain meshing, a modern graphical user interface and state-of-the-art numerical methods for the model solution. Here, the plug-flow can be directly described by a differential equation, which makes implementation much easier, also when coupling it with the 2D biofilm compartment. The computational domains were discretized with non-uniform meshes of 50 nodes in the biofilm and 300 nodes along the biofilm reactor length and bulk liquid.

First, a steady-state calculation of the solute profiles in the liquid and biofilm was performed without biofilm growth. Then, the time-dependent equations were solved

for 20 days, starting from the previously calculated steady state.

Benchmark simulations

Several benchmark simulations at initial stage (data not shown) were carried out to identify the effects on the conversion of organic matter and ammonium. The following important parameters for model development were varied: bulk liquid thickness (L_L [cm], 0.5, 1, 1.5), biofilm thickness (L_B [μm], 200, 500, 1000), biofilm density (X_B [g/L], 7.5, 15, 30), light intensity ([μmol/(m^2 s)], 3.5, 14, 56), light half-saturation coefficient ($K_{s,I,z,PH}$ [μmol/(m^2 s)], 19.2, 42, 192), and oxygen mass transfer coefficient (k_{La} [1/s], 1×10^{-4}, 2×10^{-4}, 2.7×10^{-4}).

Sensitivity analysis

From the previous parameters a subset of those that could not be measured experimentally was assessed with a sensitivity analysis. The subset was composed from the biofilm thickness, half-saturation coefficient for light, and, the oxygen mass transfer coefficient.

Model tuning

A model tuning was carried out focussing on two parameters: the gas–liquid oxygen mass transfer coefficient and the light half-saturation coefficient for phototrophs.

RESULTS AND DISCUSSION

Sensitivity analysis

The sensitivity analysis (see Table 3) revealed that the half-saturation coefficient for light and the oxygen mass transfer coefficient are the most influential parameters in this model. The mass transfer coefficient appears to be determining for the substrate conversion rate. As expected from the kinetics, the light half-saturation coefficient for phototrophs can have a large impact on the nitrogen conversion if it reaches a value similar to the light intensity applied. Thus, these parameters were adjusted to fit the measured effluent concentrations (confidential company data not presented here). The biofilm thickness was set to 500 μm since a significant impact on the COD conversion was not observed, either in the maximum or the minimum values assessed.

Model tuning

After tuning the two selected parameters, the values that fitted best the experimental results on the overall reactor performance were $k_{La}=10^{-4}$ 1/s and $K_{s,I,Ph}=28$ μmol/(m s). The initial concentration of the different species in the biofilm was also set to a value that was assumed based on experimental results: heterotrophs 5 gCOD/L, nitrifiers 13 gCOD/L, and phototrophs 19 gCOD/L. The observed

Table 3 | Sensitivity analysis results

Parameter	k_{La} 1/s		$K_{s,I,Ph}$ [μmol/(m^2 s)]		L_B [μm]	
	Default value: 1.5×10^{-4}		Default value: 38.4		Default value: 500	
Default value * factor	COD conversion %	N-NH_4^+ conversion %	COD conversion %	N-NH_4^+ conversion %	COD conversion %	N-NH_4^+ conversion %
0.5	–	–	74.96	35.97	70.56	4.78
0.6	–	–	74.77	19.59	72.46	5.38
0.7	63.53	5.42	74.72	14.96	73.11	6.08
0.8	68.21	5.52	74.66	11.54	73.29	6.65
0.9	72.37	5.86	74.54	8.96	73.32	7.08
1	74.28	7.04	74.28	7.04	74.28	7.04
1.1	74.59	8.90	73.47	5.81	73.24	7.62
1.2	74.69	10.82	71.85	5.21	73.19	7.78
1.3	74.73	12.92	70.07	4.88	73.14	7.89
1.4	–	–	68.45	4.65	73.09	7.96
1.5	–	–	67.01	4.49	73.05	8.02

Influent concentrations: COD = 400 mg/L, N-NH_4^+ = 60 mg/L.

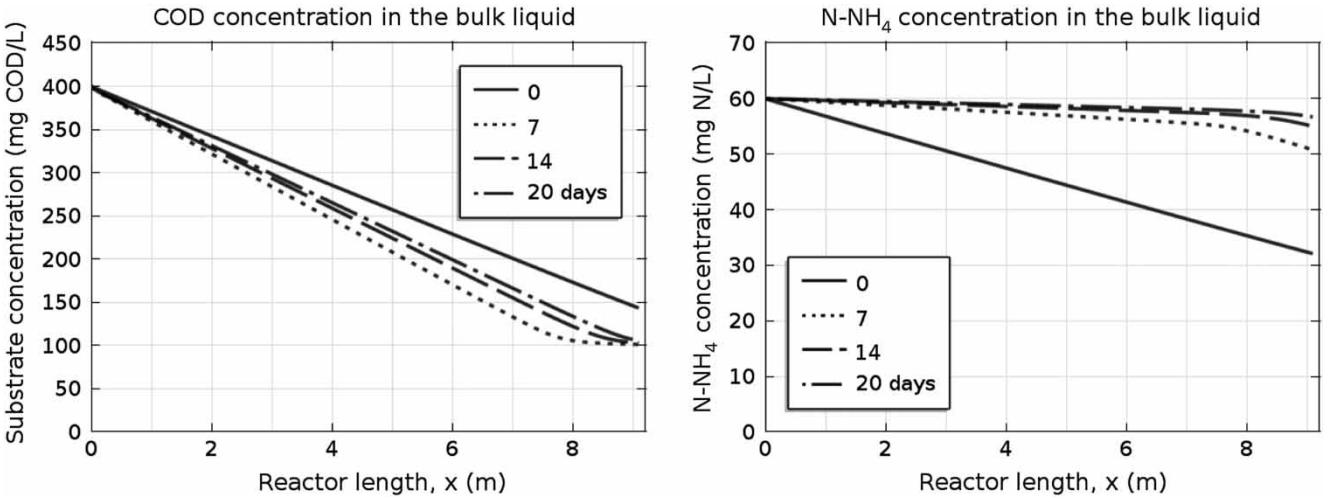

Figure 2 | Substrate and ammonia concentration in bulk liquid, over the reactor length, changing within 20 days of biofilm development. Loading rates of 6.18 gCOD/(m^2 d) (left) and 0.92 gN/(m^2 d) (right), respectively.

average density of the biofilm (37 gCOD/L) was kept constant in the model.

Concentrations in bulk liquid

For the base case simulated with the typical domestic wastewater values of 400 gCOD/m^3 (6.18 gCOD/(m^2 d)) and 60 gN/m^3 (0.92 gN/(m^2 d)) in reactor influent, the COD removal along the reactor increases in time, while the N removal declines (Figure 2). This is correlated with the change in microbial populations in the biofilm in time: the fraction of heterotrophic organisms increases in the biofilm, while phototrophs and autotrophs are gradually eliminated (Figure 3). Near the reactor inlet, a steady heterotrophic population profile establishes, in a much higher concentration than the initial one (Figure 3(a)), due to the COD availability. Near the outlet (Figure 3(b)), the heterotrophs grow only in the outer biofilm layer, because less COD is present in bulk liquid, although oxygen is still available (Figure 4).

Concentrations in the biofilm

As it was indicated in the PHOBIA model (Wolf *et al.* 2007), the majority of nitrogen removal occurred due to the nitrogen assimilation into phototrophic biomass rather than the nitrification process. The growth of nitrifiers is very limited near the inlet due to competition with phototrophs for CO_2 and with heterotrophs for O_2 (Figure 3(c)). However, at the end of the plug-flow reactor, when the organic matter reached a low concentration, the autotrophic activity becomes significant (Figure 3(d)). The maximum growth rate of the autotrophic bacteria is almost five times smaller compared to the maximum growth rate of heterotrophs. Accordingly, autotrophic biomass has a disadvantage in zones of the plug-flow reactor with more heterotrophic growth (i.e., higher COD in the inlet).

The phototrophic biomass is only moderately present along the entire reactor (Figure 3(e) and 3(f)). Experiments have shown that phototrophic biofilms grown under similar conditions have a composition that varies significantly not only along the reactor but also in different runs (Roeselers *et al.* 2006), which makes it difficult to draw definite conclusions on the population dynamics.

The oxygen profiles in the biofilm shown in Figure 4 illustrate how the oxygen penetration depth varies with position along the reactor (e.g., inlet vs outlet). Almost full oxygen penetration was achieved at the reactor end (up to 450 μm, Figure 4(b)), which corresponds with the fact that there is no biodegradable COD at the end of the reactor, but also that more phototrophic microorganisms producing O_2 are present. On the other hand, the oxygen penetration of about 150–200 μm at the inlet corresponds with the domination of heterotrophs (Figure 4(a)), well in agreement with measurements by Horn & Hempel (1995). If there is not enough phototrophic activity within the biofilm then a biofilm thickness above 200 μm does not influence substrate concentrations in the effluent. In addition, simulations show that also the oxygen mass

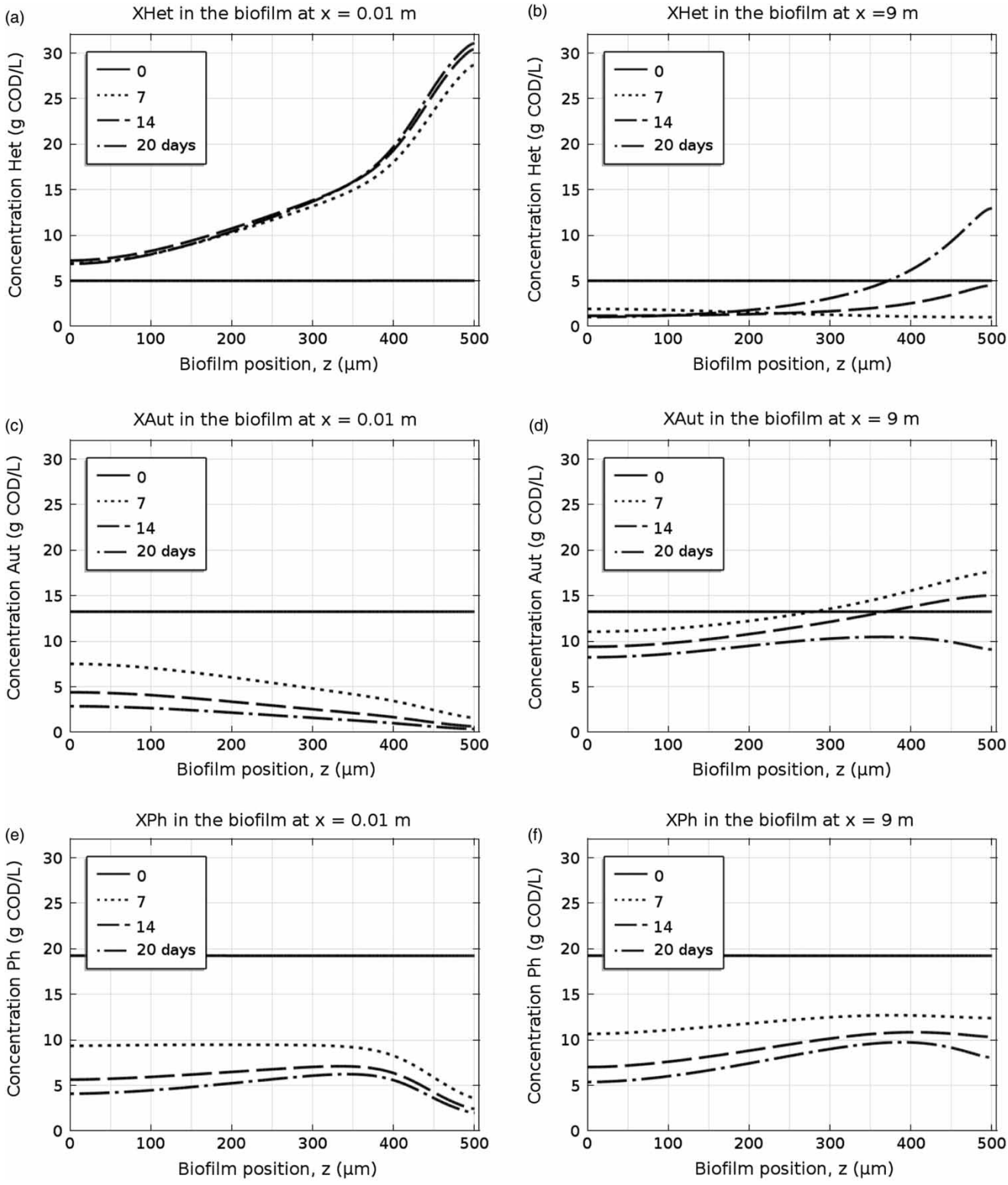

Figure 3 | Biomass concentration within biofilm at reactor inlet ($x = 0.01$ m) and outlet ($x = 9$ m).

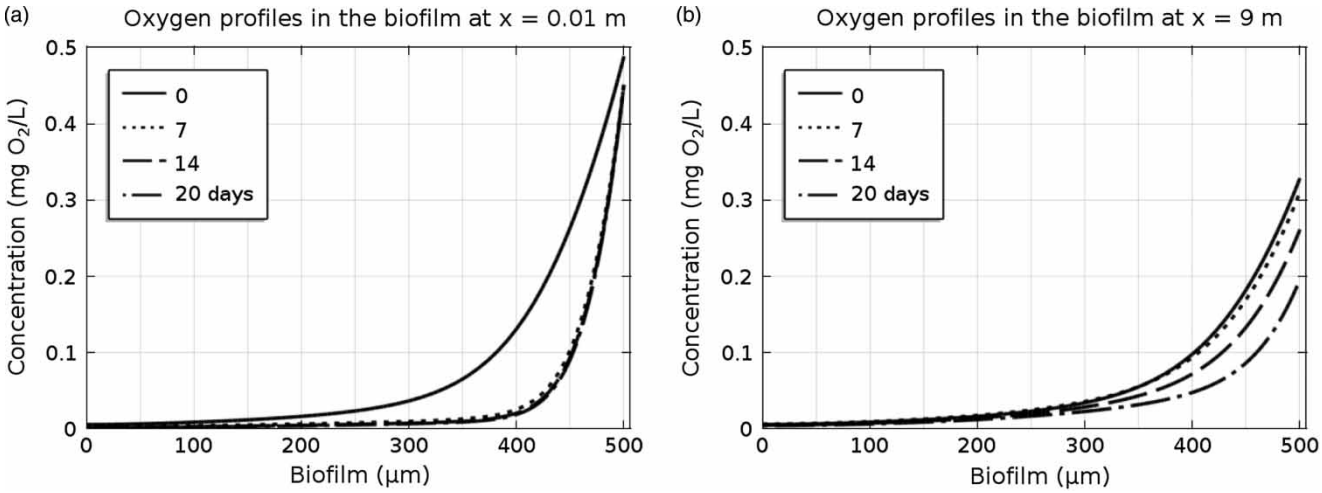

Figure 4 | Oxygen concentration within the biofilm near reactor inlet ((a), $x = 0.01$ m) and outlet ((b), $x = 9$ m) after 7, 14 and 20 days of operation.

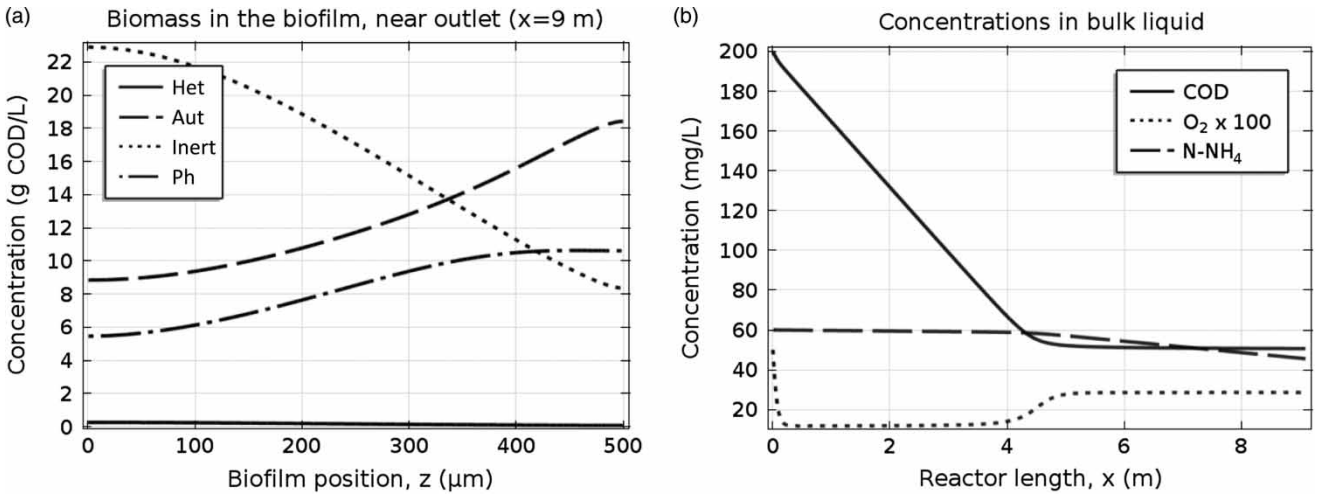

Figure 5 | (a) Biomass concentrations in the biofilm near reactor outlet ($x = 9$ m). (b) Concentration in the bulk liquid along the reactor after 20 days of operation. On the y-axis, the dissolved oxygen concentration was multiplied by 100.

transfer coefficient has a representative impact on the organic matter conversion of the system, because of the oxygen diffusion limitation.

Influent concentrations

Increased COD inlet concentration leads to lower conversions. Ammonia conversion is strictly linked to the removal of organic matter: if the COD removal is enhanced, the nitrogen removal is also improved. It was found that nitrogen removal is very limited at high organic carbon concentration (i.e., COD >200 mg/L). In this case, the heterotrophs dominate the biofilm along the whole reactor. At 200 mg COD/L in the inlet (3.09 gCOD/(m^2 d)), however, heterotrophs are only present in the first half of the flow lane and not towards the outlet (Figure 5(a)), where all biodegradable COD has already been consumed (Figure 5(b)). Accordingly, the N conversion takes place in the second half of the plug-flow reactor (Figure 5(b)).

Phototrophic activity alone is apparently not sufficient to provide enough oxygen for COD removal. Further research should investigate the actual light half-saturation coefficient to elucidate whether there is inhibition by light

of the phototrophic bacteria. Furthermore, it is necessary to find a balance between the organic loading rates (OLRs) and variable low light intensities (including day–night cycles especially for nitrogen removal) to overcome the limitations observed by the model.

CONCLUSIONS

- A systematic approach was used to build up and tune the proposed phototrophic biofilm model. The oxygen mass transfer coefficient and the phototrophic half-saturation coefficient for light were found to be sensitive parameters.
- In a plug-flow reactor configuration, the heterotrophs overgrow nitrifiers and phototrophs within the biofilm until the biodegradable COD in the liquid becomes low enough (biodegradable COD <150 mg/L, OLR $<$ 2.32 gCOD/(m^2 d)). This limits the proposed positive effect of treating wastewater with a combination of algae and bacteria under the simulated conditions.
- The mechanistic numerical model in this study was constructed to describe the dynamics of microbial groups in the biofilm along the reactor length, and to be able to make reasonable predictions of a phototrophic plug-flow reactor performance for sewage treatment.
- Simulation results revealed that nitrogen removal is very limited at organic loading rates higher than 3.09 gCOD/(m^2 d) (i.e., COD >200 mg/L) within the phototrophic biofilm reactor.
- The new generation of modeling tools incorporates the advantages of total flexibility in choosing model structure, equations and meshing, making the model construction and results representation easier along the length of the plug-flow reactor.

REFERENCES

Boelee, N. C., Temmink, H., Janssen, M., Buisman, C. J. N. & Wijffels, R. H. 2011 Nitrogen and phosphorus removal from municipal wastewater effluent using microalgal biofilms. *Water Research* **45** (18), 5925–5933.

Borde, X., Guieysse, B., Delgado, O., Muoz, R., Hatti-Kaul, R., Nugier-Chauvin, C., Patin, H. & Mattiasson, B. 2003 Synergistic relationships in algal-bacterial microcosms for the treatment of aromatic pollutants. *Bioresource Technology* **86** (3), 293–300.

Chavan, A. & Mukherji, S. 2008 Treatment of hydrocarbon-rich wastewater using oil degrading bacteria and phototrophic microorganisms in rotating biological contactor: Effect of N: P ratio. *Journal of Hazardous Materials* **154** (1–3), 63–72.

Chavan, A. & Mukherji, S. 2010 Effect of co-contaminant phenol on performance of a laboratory-scale RBC with algal-bacterial biofilm treating petroleum hydrocarbon-rich wastewater. *Journal of Chemical Technology and Biotechnology* **85** (6), 851–859.

Christenson, L. & Sims, R. 2011 Production and harvesting of microalgae for wastewater treatment, biofuels, and bioproducts. *Biotechnology Advances* **29** (6), 686–702.

De Godos, I., González, C., Becares, E., García-Encina, P. A. & Muñoz, R. 2009 Simultaneous nutrients and carbon removal during pretreated swine slurry degradation in a tubular biofilm photobioreactor. *Applied Microbiology and Biotechnology* **82** (1), 187–194.

González, C., Marciniak, J., Villaverde, S., León, C., García, P. A. & Muñoz, R. 2008 Efficient nutrient removal from swine manure in a tubular biofilm photo-bioreactor using algae-bacteria consortia. *Water Science and Technology* **58** (1), 95–102.

Henze, M., Gujer, W., Mino, T. & van Loosdrecht, M. 2000 *Activated Sludge Models ASM1, ASM2, ASM2D and ASM3*. IWA Publishing, London.

Horn, H. & Hempel, D. C. 1995 Mass transfer coefficients for an autotrophic and a heterotrophic biofilm system. *Water Science and Technology* **32** (8), 199–204.

Morgenroth, E. & Wilderer, P. A. 2000 Influence of detachment mechanisms on competition in biofilms. *Water Research* **34** (2), 417–426.

Muñoz, R. & Guieysse, B. 2006 Algal-bacterial processes for the treatment of hazardous contaminants: A review. *Water Research* **40** (15), 2799–2815.

Ohashi, A., De Silva, D. G. V., Mobarry, B., Manem, J. A., Stahl, D. A. & Rittmann, B. E. 1995 Influence of substrate C/N ratio on the structure of multi-species biofilms consisting of nitrifiers and heterotrophs. *Water Science and Technology* **32** (8), 75–84.

Pasztor, I., Thury, P. & Pulai, J. 2009 Chemical oxygen demand fractions of municipal wastewater for modeling of wastewater treatment. *International Journal of Environmental Science and Technology* **6** (1), 51–56.

Roeselers, G., Zippel, B., Staal, M., van Loosdrecht, M. & Muyzer, G. 2006 On the reproducibility of microcosm experiments – Different community composition in parallel phototrophic biofilm microcosms. *FEMS Microbiology Ecology* **58** (2), 169–178.

Roeselers, G., van Loosdrecht, M. C. M. & Muyzer, G. 2008 Phototrophic biofilms and their potential applications. *Journal of Applied Phycology* **20** (3), 227–235.

Safonova, E., Kvitko, K. V., Iankevitch, M. I., Surgko, L. F., Afti, I. A. & Reisser, W. 2004 Biotreatment of industrial wastewater by selected algal-bacterial consortia. *Engineering in Life Sciences* **4** (4), 347–353.

Schumacher, G. & Sekoulov, I. 2002 Polishing of secondary effluent by an algal biofilm process. *Water Science and Technology* **46** (8), 83–90.

Shi, J., Podola, B. & Melkonian, M. 2007 Removal of nitrogen and phosphorus from wastewater using microalgae immobilized

on twin layers: An experimental study. *Journal of Applied Phycology* **19** (5), 417–423.

Wanner, O. & Gujer, W. 1985 Competition in biofilms. *Water Science and Technology* **17** (2–3–3 pt 1), 27–44.

Wanner, O. & Reichert, P. 1996 Mathematical modeling of mixed-culture biofilms. *Biotechnology and Bioengineering* **49** (2), 172–184.

Wilkie, A. C. & Mulbry, W. W. 2002 Recovery of dairy manure nutrients by benthic freshwater algae. *Bioresource Technology* **84** (1), 81–91.

Wolf, G., Picioreanu, C. & van Loosdrecht, M. C. M. 2007 Kinetic modeling of phototrophic biofilms: The PHOBIA model. *Biotechnology and Bioengineering* **97** (5), 1064–1079.

First received 3 January 2014; accepted in revised form 11 August 2014. Available online 23 August 2014